

Zwitterion-Stabilized Silica Nanoparticles: Toward Nonstick Nano

Zaki G. Estephan, Jad A. Jaber, and Joseph B. Schlenoff*

Department of Chemistry and Biochemistry, The Florida State University, Tallahassee, Florida 32306, United States

Received August 3, 2010. Revised Manuscript Received September 23, 2010

Using a short-chain zwitterionic organosiloxane, silica nanoparticles were stabilized against aggregation by high ionic strength and/or proteins. Turbidimetry and dynamic light scattering showed that “zwitterated” nanoparticles did not exhibit a significant increase in hydrodynamic radius. When challenged with 3 M NaCl or 50% fetal bovine serum, aggregation was inhibited for at least 24 h, longer with mild heat treatment, which produced nanoparticles with zero net surface charge. These findings suggest “zwitteration” of silica-capped nanoparticles provides excellent stability for *in vivo* circulation diagnostics and therapies.

Introduction

Nanoparticles show promise for selective *in vivo* targeting of cancer cells in addition to their use in contrast agents and diagnosis.^{1,2} In the case of cancer, nano dimensions permit enhanced transport across the fenestrated endothelial cell lining of tumor vascular tissue to access tumor masses.³ For efficient and targeted nanoparticle transport, the surface chemistry must provide both targeting ligands and passivation against nonspecific uptake.⁴ The latter property requires minimal cytotoxicity of the nanocarrier while it evades the immune system by avoiding opsonization (the process of tagging nanoparticles with proteins for destruction by phagocytes) and thus early clearance from blood circulation.^{4,5}

Biocompatibility and reduced cytotoxicity are often achieved by core/shell or core/shell/shell geometries. Numerous core compositions, tailored to the application, have been described, such as fluorescent II–VI or III–V quantum dots including CdSe/CdS or CdSe/ZnS,^{6,7} metallic nanoparticles like Ag or Au,^{8–10} or magnetic materials such as Fe₃O₄.^{11,12} The shell is often a layer of silica, which offers relative biocompatibility (bioinertness) and a broad palette of well-understood surface chemistry, allowing further functionalization.¹³ In addition to reducing cytotoxicity, silica shells also play a broad role in stabilizing nanocrystals such

as Pd,¹⁴ improving photoluminescent stability of fluorescent sensors and biomarkers,^{15,16} and in hybrid organic/inorganic materials.¹⁷

In a physiological environment, nonspecific adsorption of proteins to the surface of nanoparticles controls their fate.^{4,18} For example, it has been reported that the adsorption of IgG and fibrinogen promotes phagocytosis by the reticuloendothelial system, resulting in rapid clearance of the particles from blood circulation and concentration in the liver and spleen.⁴ The adsorption of ApoE, on the other hand, enhances transport across the blood–brain barrier.⁴ In all cases, adsorption has been found to depend on many factors, including size, shape, surface charge, and surface chemistry.^{4,5,19} Protein adsorption increases the hydrodynamic radius of the particle, a factor that must be avoided if the effect of size on uptake is under study.⁴ Thus, in engineering a new particle, minimizing nonspecific protein adsorption is required in order to achieve increased serum half-life and to avoid delivery to nontargeted tissues.

The most widely used method to prevent opsonization is via grafting the nanoparticle surface with poly(ethylene glycol), PEG, or a PEG derivative,² though other polymers such as poly(vinyl alcohol), poly(ethylloxazoline), and poly(vinylpyrrolidone) have been reported.²⁰ However, PEG does not completely eliminate protein adsorption, as fibrinogen, apolipoprotein E, and IgG adsorption have been reported on surfaces coated with PEG moieties.^{21,22} In addition, the stability of PEG is compromised in the presence of oxygen and transition metal ions due to oxidation,²³ and although it is able to resist protein adsorption at

*Corresponding author. E-mail: schlen@chem.fsu.edu.

(1) Han, G.; Ghosh, P.; Rotello, V. M. *Nanomedicine* **2007**, *2*, 113–123.

(2) Thierry, B.; Zimmer, L.; McNiven, S.; Finnie, K.; Barbé, C.; Griessert, H. J. *Langmuir* **2008**, *24*, 8143–8150.

(3) Greish, K. J. *Drug Targeting* **2007**, *15*, 457–464.

(4) Aggarwal, P.; Hall, J. B.; McLeland, C. B.; Dobrovolskaia, M. A.; McNeil, S. E. *Adv. Drug Delivery Rev.* **2009**, *61*, 428–437.

(5) Perrault, S. D.; Walkey, C.; Jennings, T.; Fischer, H. C.; Chan, W. C. W. *Nano Lett.* **2009**, *9*, 1909–1915.

(6) Zhu, M. D.; Han, J. J.; Li, A. D. Q. *J. Nanosci. Nanotechnol.* **2007**, *7*, 2343–2348.

(7) Graf, C.; Dembski, S.; Hofmann, A.; Rühl, E. *Langmuir* **2006**, *22*, 5604–5610.

(8) Baida, H.; Billaud, P.; Marhaba, S.; Christofilos, D.; Cottancin, E.; Crut, A.; Lermé, J.; Maioli, P.; Pellarin, M.; Broyer, M.; Del Fatti, N.; Vallée, F.; Sánchez-Iglesias, A.; Pastoriza-Santos, I.; Liz-Marzán, L. M. *Nano Lett.* **2009**, *9*, 3463–9.

(9) Liz-Marzán, L. M.; Giersig, M.; Mulvaney, P. *Langmuir* **1996**, *12*, 4329–4335.

(10) Rodríguez-Fernández, J.; Pastoriza-Santos, I.; Pérez-Juste, J.; de Abajo, F. J. G.; Liz-Marzán, L. M. *J. Phys. Chem. C* **2007**, *111*, 13361–13366.

(11) Atarashi, T.; Kim, Y. S.; Fujita, T.; Nakatsuka, K. *J. Magn. Magn. Mater.* **1999**, *201*, 7–10.

(12) Tartaj, P.; González-Carreño, T.; Serna, C. J. *J. Phys. Chem. B* **2003**, *107*, 20–24.

(13) Liz-Marzán, L. M.; Mulvaney, P. *J. Phys. Chem. A* **2003**, *107*, 7312–7326.

(14) Park, J. N.; Forman, A. J.; Tang, W.; Cheng, J. H.; Hu, Y. S.; Lin, H. F.; McFarland, E. W. *Small* **2008**, *4*, 1694–1697.

(15) Santra, S.; Liesenfeld, B.; Dutta, D.; Chatel, D.; Batich, C. D.; Tan, W.; Moudgil, B. M.; Mericle, R. A. *J. Nanosci. Nanotechnol.* **2005**, *5*, 899–904.

(16) Burns, A. A.; Vider, J.; Ow, H.; Herz, E.; Penate-Medina, O.; Baumgart, M.; Larson, S. M.; Wiesner, U.; Bradbury, M. *Nano Lett.* **2009**, *9*, 442–448.

(17) Fujii, S.; Armes, S. P.; Binks, B. P.; Murakami, R. *Langmuir* **2006**, *22*, 6818–6825.

(18) Owens, D. E.; Peppas, N. A. *Int. J. Pharm.* **2006**, *307*, 93–102.

(19) Cho, M. J.; Cho, W. S.; Choi, M.; Kim, S. J.; Han, B. S.; Kim, S. H.; Kim, H. O.; Sheen, Y. Y.; Jeong, J. Y. *Toxicol. Lett.* **2009**, *189*, 177–183.

(20) Rabinow, B. E.; Ding, Y. S.; Qin, C.; McHalsky, M. L.; Schneider, J. H.; Ashline, K. A.; Shelbourn, T. L.; Albrecht, R. M. *J. Biomater. Sci., Polym. Ed.* **1994**, *6*, 91–109.

(21) Gref, R.; Lück, M.; Quellec, P.; Marchand, M.; Dellacherie, E.; Harnisch, S.; Blunk, T.; Müller, R. H. *Colloids Surf., B* **2000**, *18*, 301–313.

(22) Kim, H. R.; Andrieux, K.; Delomenie, C.; Chacun, H.; Appel, M.; Desmaële, D.; Taran, F.; Georgin, D.; Couvreur, P.; Taverna, M. *Electrophoresis* **2007**, *28*, 2252–2261.

(23) Luk, Y. Y.; Kato, M.; Mrksich, M. *Langmuir* **2000**, *16*, 9604–9608.

room temperature, its repulsive properties are diminished above 35 °C.²⁴ Another disadvantage is the increase in hydrodynamic size upon PEGylation. For example, in an attempt to study the renal cutoff size for the filtration of nanoparticles, Choi et al.²⁵ reported that they were unable to synthesize a PEG-coated CdSe/ZnS quantum dot smaller than 10 nm.

Zwitterions, which make up the majority of typical mammalian cell surfaces, are known to be effective in reducing protein adsorption.²⁶ Holmlin et al. reported that self-assembled thiol monolayers terminated with zwitterions were able to resist protein adsorption onto gold.²⁷ Recently, Matsuura et al.²⁸ and Jia et al.²⁹ have separately reported water-soluble, aggregation-resistant, gold and silica colloids, respectively, having a carboxybetaine polymer on the surface. However, the grafting of the polymer onto the surface resulted in an increase in the hydrodynamic diameter by a factor of 2 in the case of silica nanoparticles.²⁹ Our laboratory has previously reported the stabilization of gold nanoparticles with a zwitterion disulfide ligand.³⁰ The water-soluble gold colloids showed a minor increase in size (around 1 nm) before and after exchanging the citrate ligand with the zwitterion disulfide and were stable in protein solutions and at high salt concentration with no evidence of protein adsorption. In a similar approach, Muro et al. reported the synthesis of a bidentate sulfobetaine for *in vitro* stabilization of quantum dots.³¹

In the present work, we report the synthesis of a small sulfobetaine siloxane and the stabilization of silica nanoparticles through straightforward aqueous siloxane chemistry. Adding a dense zwitterion coating to silica nanoparticles did not measurably increase their size, yet exceptional stability in solutions of concentrated salt or protein was observed.

Experimental Section

Materials. Ludox TM-40 colloidal silica, 40 wt % suspension in water was used as received from Sigma-Aldrich. Fetal bovine serum (VWR) and lysozyme (from chicken egg white, protein $\geq 90\%$, Sigma-Aldrich) were stored at $-20\text{ }^{\circ}\text{C}$. Sodium phosphate monobasic (ACS grade), sodium phosphate (ACS grade), acetone (HPLC grade), and NaCl (ACS grade) were from Fisher Scientific. (*N,N*-dimethyl-3-aminopropyl)trimethoxysilane was purchased from Gelest and stored under nitrogen. Propane sultone was obtained from TCI America.

Synthesis of 3-(Dimethyl(3-(trimethoxysilyl)propyl)ammonio)propane-1-sulfonate. SBS. The synthesis of zwitterion siloxane, SBS, was adapted from Litt et al.³² To 4.45 g of propane sultone in 37 mL of acetone under Ar was added 7.5 g of (*N,N*-dimethyl-3-aminopropyl)trimethoxysilane (Figure S1, Supporting Information). The reaction was stirred vigorously for 6 h. The white precipitate was collected by vacuum filtration and washed twice with acetone. The white solid was dried and stored under Ar. Yield 90%.

¹H NMR 300 MHz *d*-DMSO is presented in Table S1.

(24) Efremova, N. V.; Sheth, S. R.; Leckband, D. E. *Langmuir* **2001**, *17*, 7628–7636.

(25) Choi, H. S.; Liu, W.; Misra, P.; Tanaka, E.; Zimmer, J. P.; Ipe, B. I.; Bawendi, M. G.; Frangioni, J. V. *Nature Biotechnol.* **2007**, *25*, 1165–1170.

(26) West, S. L.; Salvage, J. P.; Lobb, E. J.; Armes, S. P.; Billingham, N. C.; Lewis, A. L.; Hanlon, G. W.; Lloyd, A. W. *Biomaterials* **2004**, *25*, 1195–1204.

(27) Holmlin, R. E.; Chen, X. X.; Chapman, R. G.; Takayama, S.; Whitesides, G. M. *Langmuir* **2001**, *17*, 2841–2850.

(28) Matsuura, K.; Ohno, K.; Kagaya, S.; Kitano, H. *Macromol. Chem. Phys.* **2007**, *208*, 862–873.

(29) Jia, G. W.; Cao, Z. Q.; Xue, H.; Xu, Y. S.; Jiang, S. Y. *Langmuir* **2009**, *25*, 3196–3199.

(30) Rouhana, L. L.; Jaber, J. A.; Schlenoff, J. B. *Langmuir* **2007**, *23*, 12799–12801.

(31) Muro, E.; Pons, T.; Lequeux, N.; Fragola, A.; Sanson, N.; Lenkei, Z.; Dubertret, B. *J. Am. Chem. Soc.* **2010**, *132*, 4556–4557.

(32) Litt, M.; Matsuda, T. *J. Appl. Polym. Sci.* **1975**, *19*, 1221–1225.

Addition of Zwitterion Siloxane to Silica Nanoparticles.

The appropriate amount of zwitterion siloxane previously dissolved in water was added to 10 wt % final concentration Ludox nanoparticles under vigorous stirring. The pH remained at ~ 9 . The mixture was stirred for 6 h either at room temperature (rt) or at $80 \pm 5\text{ }^{\circ}\text{C}$. The solution was then centrifuged at 13 000 rpm (Avant J-25, Beckman Coulter centrifuge) for 15 min. The centrifugate collected, redispersed in 10 mL of H₂O, and washed again twice. The final centrifugate was collected and dried under vacuum at 20 °C.

The reaction was also performed in the presence of ammonia. 0.5 mL of ammonia was added prior to heating at $80 \pm 5\text{ }^{\circ}\text{C}$.

Nanoparticle Characterization. The hydrodynamic radius of the zwitterionic silica was measured by dynamic light scattering at 690 nm (DAWN EOS, Wyatt Technology). Approximately 100 μL of the 10% silica solution was dispersed in 10 mL of PBS (10 mM, 0.14 M NaCl, pH 7.4). Samples were injected into the flow cell using a syringe pump at a flow rate of 10 mL/h, and measurements were recorded for 1 min at a collection interval of 2 s. Results are reported in Table S2.

The addition of the zwitterion siloxane to the siloxane surface was confirmed with ¹³C solid-state NMR. CP/MAS experiments were performed at 125 MHz at an angle of 54.74° and 15 kHz spinning rate using a Varian INNOVA 500 MHz wide-bore spectrometer. Samples were carefully washed by centrifugation three times at 13 000 rpm for 30 min and dried under vacuum. Table S1 shows the assigned peaks.

The amount of zwitterion siloxane on the silica surface was followed qualitatively using diffuse reflectance infrared Fourier transform (DRIFT) spectroscopy. Dried nanoparticles were gently ground and mixed with KBr powder. Spectra were collected under N₂ using a Nicolet Avatar 360 FTIR with a DTGS-KBr detector. 1000 scans were performed on each sample at 4.0 cm⁻¹ resolution, and spectra were referenced against a KBr background.

Quantitative determination of zwitterion siloxane on silica surface was performed via thermogravimetric analysis, TGA (TA Instruments Q50). Approximately 10 mg of dried nanoparticles was placed in a platinum cup inside an oven continuously purged with N₂ at a flow rate of 100 mL/min. The temperature of the oven was ramped to 105 °C, where it was held constant for 20 min to ensure the desorption of adsorbed water. Finally, the temperature was ramped to 800 at 10 °C/min. An empty sample cup was run as a background.

Zeta potential measurements were performed on a Malvern Instruments Zetasizer ZEN 3600 by measuring the electrophoretic mobility of 0.25% w/v aqueous dispersions in 0.01 M NaCl as a function of pH. A Malvern MP2T titrator was used to gradually change the pH from 10 down to 2 by the addition of HCl_{aq} over 150 min. Zeta potentials were averaged over a minimum of 35 runs.

Hydrolysis of Zwitterion Siloxane. The hydrolysis rate of the zwitterion siloxane in water was followed with ¹H NMR. Measurements were performed at rt in D₂O with a Bruker Ultrashield 600 MHz NMR. Figure S3 shows NMR spectra collected at different intervals for 35 mg of zwitterion siloxane in 600 μL of D₂O. A few seconds after the addition of the zwitterion siloxane to water the spectrum shows a prominent peak at δ 3.6 ppm attributed to the methoxy groups. As time proceeds, this peak starts to decrease and another peak appears at δ 3.3 ppm from free methanol. In addition, an upfield shift, from δ = 0.8 ppm to 0.66 ppm, is observed for the methylene group directly bonded to the silicon atom. This upfield shift is another indication of the Si–O–CH₃ hydrolysis. The rate of hydrolysis was followed by monitoring the decrease in peak area for the methoxy group and the appearance of the methanol as well as by monitoring the change in the signal of the methyl group connected to the silicon atom as it shifts upfield. All integrated signals were normalized to the theoretical nine methoxy hydrogens. As shown in Figure S4, the half-life for hydrolysis is about an hour, indicating efficient hydrolysis in water at rt.

Resistance to Salt- or Protein-Induced Aggregation. Turbidimetry was used to study the effect of salt or protein on the

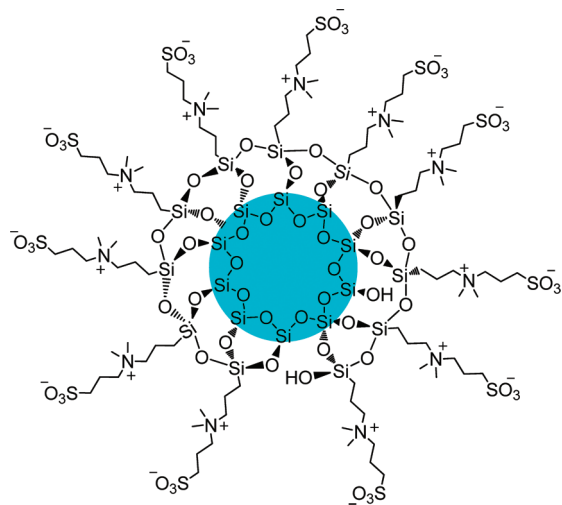


Figure 1. Cartoon of a silica nanoparticle decorated with sulfobetaine siloxane (zwitterion).

aggregation of zwitterated nanoparticles. Turbidimetry was collected using a Varian Cary 100 UV/vis double-beam spectrophotometer. Samples were placed in disposable cuvettes, and measurements were collected at 500 nm. In all experiments, nanoparticle concentration was 2% w/v. The setup was temperature controlled, and samples were magnetically stirred.

For stability in salt solutions, nanoparticles were first dispersed in 10 mM phosphate buffer pH 7.4 at 25 °C. NaCl stock solution was then added to samples, including the blank solution.

For stability in FBS, nanoparticles were dispersed in PBS (10 mM, 0.14 M NaCl, pH 7.4) at 37 °C. FBS was then added to the sample cuvette and to the reference cell. The final FBS concentration was 50% v/v.

The effect of lysozyme on the hydrodynamic diameter of the particles was assessed using dynamic light scattering (DLS). Experiments were performed on DynaPro instrument (Wyatt Technology). 1 mL of 3.5 mg/mL of lysozyme solution was added to 3.8 mg of nanoparticles in 2.5 mL of PBS (10 mM, pH 7.4), and the final solution was measured with DLS at 37 °C and compared to the original sample with no lysozyme.

In the case of untreated silica nanoparticles, the solution became milky upon incubation with lysozyme. The signal from this solution oversaturated the detector, and therefore a set of dilutions were performed until proper signal was obtained. The laser power was adjusted to 10%, and the acquisition time was set to 30 s. No turbid solution was observed for the zwitterion treated silica nanoparticles which had 1.7 μmol zwitterion/ m^2 (or μmol Zwi/ m^2). The solution was left at room temperature for 6 h followed by heating at 80 °C for 6 h. The final solution was extensively dialyzed against nanopure water for 3 days. The final concentration of the dialyzed sample was measured to be 7.55% w/w. Following the above procedure, the hydrodynamic radius was measured before and after lysozyme addition. The laser power was set to 100%, and the acquisition time was 10 s.

Results and Discussion

Ring-opening addition of propane sultone by aminoalkylsiloxane was used to synthesize the highly water-soluble SBS, 3-(dimethyl-(3-(trimethoxysilyl)propyl)ammonio)propane-1-sulfonate.

Ludox TM-40, a widely available and commonly used silica colloid, was employed as a model nanoparticle to study the effect of the zwitterion coating. SBS was added to the silica nanoparticles in various amounts to determine the minimum surface coverage needed to confer stability on the particles in salt and protein media. Coverage was determined using the surface area

reported by the manufacturer ($140 \text{ m}^2 \text{ g}^{-1}$) and 4.9 silanol groups per nm^2 of silica surface,³³ or $8 \mu\text{mol m}^{-2}$.³⁴

Zwitterion dissolved in a minimum of water was added directly to stirred 10 wt % solutions of 17 nm (hydrodynamic radius) silica at rt. The mixture was stirred at rt, or under heating, for 6 h, after which unbound zwitterion was removed by centrifugation. To confirm the presence of the zwitterion siloxane on the surface, ^{13}C solid-state NMR (SSNMR) was collected before and after surface treatment as well as for the free zwitterion siloxane (Figure 2 and Table S1). No signals were observed for the untreated silica colloids, consistent with the absence of any adsorbed ligands or surfactants. The zwitterion siloxane showed a set of broad peaks that are assigned in Figure 2. The most relevant signal is at δ 49 ppm with a shoulder at δ 46 ppm. These correspond to the methoxy carbons directly attached to the silicon atom and the methylene carbon attached to the sulfonate group, respectively. The SSNMR of the “zwitterated”³⁵ silica (SiZwi) nanoparticle resembles that of the zwitterion reagent with the major exception being the disappearance of the methoxy peak at δ 49 ppm in favor of the methylene group at δ 47 ppm, consistent with zwitterion hydrolysis.

Different amounts of zwitterion were added to the silica nanoparticles, and the addition was followed using spectroscopic and thermogravimetric (TGA) analysis. Previous work on the addition of siloxanes to silica^{36–38} has shown the hydrolysis of organosiloxane in aqueous medium is fast, and thus dimers and polymers may form in solution before deposition on the surface, which leads to a polymeric network, or blanket, on the silica. Figure 2 represents various monolayer modes of attachment of a trialkoxysiloxane.

The hydrodynamic radii, R_h , of treated and bare nanoparticles were compared using DLS in PBS at pH 7.4 at 20 °C. No measurable change in R_h was observed on surface silylation (Table S2). Jia et al. reported an increase in the hydrodynamic diameter by a factor of 2 for silica nanoparticles decorated with a zwitterion polymer,²⁹ which was attributed to the bulk of the grafted polymer. In our case, the 1.3 nm length of the SBS was clearly insufficient to produce a measurable increase in nanoparticle radius, making this molecule an attractive alternative for passivating surfaces without perturbing dimensions.

The amount of zwitterion siloxane deposited on the silica surface was followed qualitatively by DRIFT and quantitatively by TGA. The bulk Si–O–Si combination band at 1870 cm^{-1} served as an internal reference.^{38,39} Figure S2A compares the DRIFT spectrum of bare silica nanoparticles and $1.0 \mu\text{mol}$ Zwi/ m^2 SiZwi. The untreated silica shows a set of peaks characteristic of a silica surface. These are 1100 and 1870 cm^{-1} attributed to Si–O–Si absorption, the broad band at 3500 cm^{-1} , and the medium band at 1630 cm^{-1} corresponding to the stretching and bending vibrations of OH groups, the absorption band at 3660 cm^{-1} assigned to two vicinal silanol groups involved in H-bonding, and the sharp band at 1740 cm^{-1} attributed to the isolated non-hydrogen-bonded Si–OH groups. The SBS-treated surface shows all of the above peaks in addition to $-\text{CH}_2$ bending at 725 cm^{-1} , Si–O–C at 1420 cm^{-1} , $-\text{CH}_2$ scissoring at 1485 cm^{-1} ,

(33) Zhuravlev, L. T. *Langmuir* **1987**, *3*, 316–318.

(34) Sunseri, J. D.; Gedris, T. E.; Stiegman, A. E.; Dorsey, J. G. *Langmuir* **2003**, *19*, 8608–8610.

(35) The term “zwitterated” silica or “zwitterated” nanoparticle will refer to a nanoparticle whose surface has been treated to contain a zwitterionic functionality. In this work it specifically refers to a nanoparticle having the sulfobetaine siloxane on its surface.

(36) Van Der Voort, P.; Vansant, E. F. *Polym. J. Chem.* **1997**, *71*, 550–567.

(37) Howarter, J. A.; Youngblood, J. P. *Langmuir* **2006**, *22*, 11142–11147.

(38) Chen, T. M.; Brauer, G. M. *J. Dent. Res.* **1982**, *61*, 1439–1443.

(39) Ek, S.; Iiskola, E. I.; Niinistö, L.; Vaittinen, J.; Pakkanen, T. T.; Keränen, J.; Auroux, A. *Langmuir* **2003**, *19*, 10601–10609.

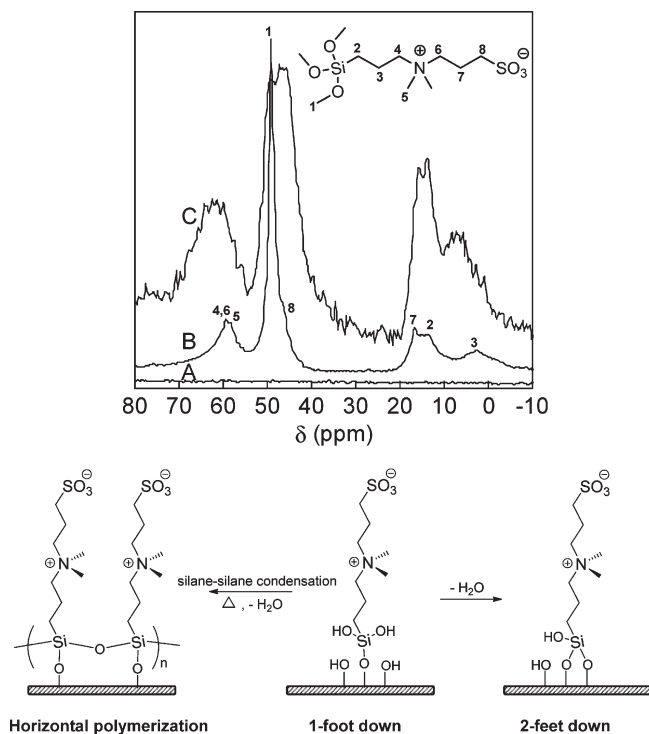


Figure 2. (upper) ^{13}C CP/MAS solid-state NMR of bare silica nanoparticle (A), free zwitterion siloxane SBS (B), and zwitterated silica nanoparticle (C). The methoxy peak in the free SBS at δ 49 ppm (peak 1) is not present in the zwitterated silica nanoparticle indicative of its hydrolysis. Inset shows the structure of the unhydrolyzed zwitterion (SBS). (lower) Different possible associations of the zwitterion siloxane to the silica surface, with one or two feet down, or horizontal polymerization (a structure with three feet down is generally discounted in the literature).

and $-\text{CH}_2$ stretching vibrations between 2900 and 3000 cm^{-1} . The 1485 cm^{-1} band was ratioed to the internal Si—O—Si reference (A_{1485}/A_{1870}) to follow the extent of surface reaction. Figure 3A shows that the surface concentration of zwitterion increases as the amount of zwitterion added to the solution increases, saturating as the amount of zwitterion added approaches 3 μmol Zwi/ m^2 . The fact that the surface coverage plateaus while excess zwitterion siloxane is added to solution suggests an absence of polymeric 3-dimensional networks of siloxane implied in other organosilane reagents.³⁶

TGA (Figure S2B) provided more quantitative data on surface coverage. A trend similar to that obtained with DRIFT was observed, where the surface amount increased with an increase in the added amount and then saturated at 1.7 μmol Zwi/ m^2 (Figure 3B). Assuming all methoxy groups hydrolyze before addition to the surface and that each zwitterion binds to one surface silanol and one other zwitterion siloxane as depicted in Figure 1, the amount of zwitterion loaded onto the surface may be calculated. As seen in Figure 3B, all zwitterion added to solution ends up on the surface of the nanoparticle at low coverage, but deviation from stoichiometry (solid line in Figure 3B) occurs above about 1 μmol Zwi/ m^2 and the surface concentration saturates at about 2 μmol Zwi/ m^2 .

Classical variables in the coating of silica surfaces with siloxanes include temperature and the presence of base. For example, heating is reported to increase the amount of bound siloxanes.³⁷ We thus heated some reaction mixtures at 80 °C for 6 h following the addition of SBS. While heating does not have a significant effect on coverage (Figure 3B), it does improve long-term stability and reduces the zeta potential, as shown below. This is consistent

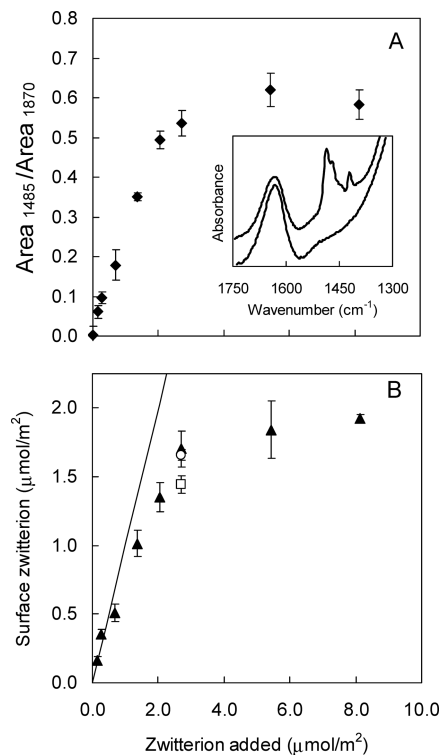


Figure 3. Amount of surface zwitterion as a function of zwitterion added to silica nanoparticles. (A) Area ratio of $-\text{CH}_2$ scissoring at 1485 cm^{-1} to Si—O—Si combination band (1870 cm^{-1}) from DRIFT. Inset: DRIFT spectra showing the appearance of 1485 cm^{-1} peak upon zwitteration. Lower spectrum is for bare silica, and upper spectrum is for 1.7 μmol Zwi/ m^2 . (B) Surface coverage from TGA for the addition at room temperature (\blacktriangle), at 80 °C (\circ), and at 80 °C with NH_3 added (\square). Solid line represents a stoichiometric reaction of SBS with surface.

with earlier findings on other trialkoxysilanes, where better stability was observed in aqueous media on *in situ* heating due to enhanced horizontal polymerization and reduced hydrolytic cleavage.^{40,41}

Some of the nanoparticles were heated at 80 °C with ammonia, which is known to catalyze surface condensation reactions resulting in higher coverage.^{36,42} In the present case, base addition proved to be counterproductive: the zwitterion surface coverage decreased (Figure 3B), probably due to the fact that siloxane hydrolysis was sufficiently fast in aqueous media, compared to organic solvents.³⁶ The kinetics for the hydrolysis of the SBS methoxy group, followed at rt in D_2O , revealed a half-life of about an hour (Figures S3 and S4).

Hydrolysis of SBS by itself in water or buffer yielded no detectible particle formation. In fact, electrospray ionization mass spectroscopy of the hydrolyzed solution showed only monomeric zwitterion triol (the hydrolysis product). Nanoparticles added to this solution formed SiZwi indistinguishable from those produced by adding SBS. Thus, the reaction of silica surface appears to be exceptionally well behaved, requiring no catalyst, producing an approximate monolayer, and yielding no oligomeric or polymeric byproducts.

The effect of zwitteration on the surface charge was assessed by measuring the zeta potential in 0.01 M NaCl solution at different

(40) Pasternack, R. M.; Amy, S. R.; Chabal, Y. J. *Langmuir* **2008**, *24*, 12963–12971.

(41) Smith, E. A.; Chen, W. *Langmuir* **2008**, *24*, 12405–9.

(42) Blum, F. D.; Meesiri, W.; Kang, H. J.; Gambogi, J. E. *J. Adhes. Sci. Technol.* **1991**, *5*, 479–496.

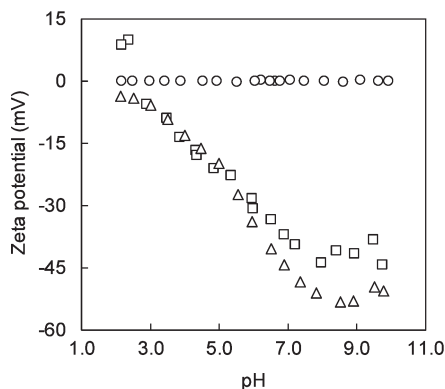


Figure 4. Zeta potential measurement of 0.25% w/v aqueous dispersion in 0.01 M NaCl as a function of pH: (□) untreated silica, (Δ) 1.7 $\mu\text{mol Zwi/m}^2$ SiZwi prepared at room temperature, and (○) 1.7 $\mu\text{mol Zwi/m}^2$ SiZwi prepared at 80 °C.

pH values (Figure 4). The surface potential profile for untreated silica nanoparticles agreed well with the large body of literature where a reduction in zeta potential is observed from ca. -40 mV at pH 9 to almost 0 at pH 2.⁴³ SiZwi prepared at rt shared a similar profile to that of the parent silica. Surface charge of these samples indicates free, dissociated silanols, as might be expected from the “one foot down” model in Figure 2. Under standard theories (e.g., DLVO) of colloid stability, the net negative surface charge at all measured pH values caused interparticle repulsion.⁴⁴ When screened by high salt concentrations, non-DLVO interactions, such as steric repulsions due to a strongly hydrated surface layer, may come into play. In contrast, no surface charge was measured for the heat-treated SiZwi over the entire pH range, consistent with the horizontal 2-dimensional polymerization arrangement in Figure 2. The stability of this nanoparticle, despite the absence of surface charge, was exceptional and again attributable to non-DLVO repulsive forces.⁴⁴

Silica nanoparticles are known to aggregate in the presence of salt.⁴³ We therefore studied the aggregation behavior of 2% w/v nanoparticles with different coverages of zwitterion siloxane in 0.5 M NaCl in pH 7.4 phosphate buffer at 25 °C over a period of 15 days. As seen in Figure 5A, in the absence of zwitterion, the absorbance, indicating aggregation, reached a plateau after 3 days. Aggregation was delayed, but not suppressed, by 0.16 and 0.35 $\mu\text{mol Zwi/m}^2$. Above 0.51 $\mu\text{mol Zwi/m}^2$ aggregation was no longer observed, even after 15 days. As a severe salt challenge, the stability of nanoparticles coated with 1.0 $\mu\text{mol Zwi/m}^2$ was evaluated in 3 M NaCl. Untreated silica nanoparticles aggregated in minutes whereas the zwitterated nanoparticles showed no increase in absorbance for the full period of study (Figure S5) reflecting the high stability of the latter system even under harsh salt conditions. Our results are in agreement with the data of Rouhana et al.³⁰ and Muro et al.,³¹ where sulfobetaine-capped nanoparticles were found to be stable in high saline media.

The stability of zwitterated nanoparticles was also studied in 50% FBS, which was selected to more closely approximate the complexity of the environment to which the nanoparticles would be exposed in an *in vivo* circulating study. Figure 5B compares turbidimetry of untreated and treated (1.0 $\mu\text{mol Zwi/m}^2$) silica nanoparticles in 50% buffered FBS. Untreated silica nanoparticles aggregated rapidly, while zwitterated nanoparticles showed

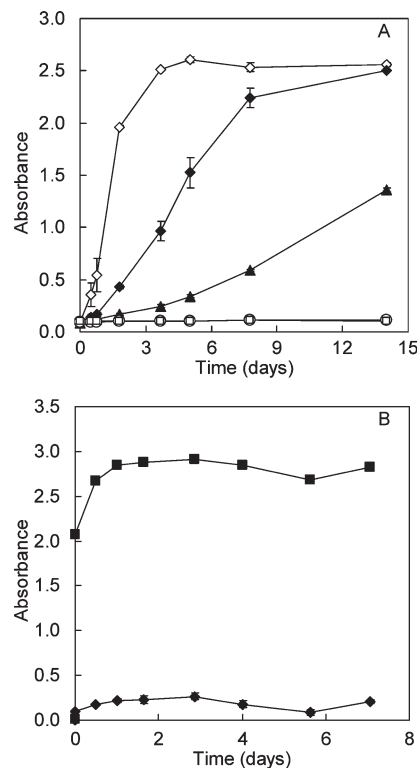


Figure 5. Turbidimetry study at $\lambda = 500$ nm showing the stability of untreated and SBS-treated silica colloid. (A) In 0.5 M NaCl buffered at pH 7.4 at 25 °C: untreated silica (◇), SiZwi corresponding to 0.16 (◆), 0.35 (▲), 0.51 (□), and 1.0 $\mu\text{mol Zwi/m}^2$ (○). (B) In 50% v/v FBS in PBS (pH 7.4) at 37 °C: untreated SiO_2 (■) and 1.0 $\mu\text{mol Zwi/m}^2$ SiO_2 (◆). Nanoparticle concentration 2% w/v.

almost no evidence of aggregation for days, even in these high levels of serum.

After heating, the stability of the nanoparticles was improved when tested in the presence of high salt concentration and high serum levels. A comparison between samples prepared with heat and another with no heat (Figure S6) revealed that the heated sample resists aggregation over longer periods, especially when the system contained elevated serum levels. We believe that heating transforms surface binding from one foot down (Figure 2) to polymerized, thus preventing hydrolytic cleavage.

In a final test, DLS was used as a sensitive probe of the adsorption of lysozyme, a positively charged “sticky” protein ($3.0 \times 3.0 \times 4.5 \text{ nm}^3$),⁴⁵ which adsorbs readily to negatively charged silica surfaces. The adsorption was followed by measuring the hydrodynamic radius of the particle on incubation with lysozyme. On addition of the protein to the untreated silica colloids, the solution turned white. The hydrodynamic radius increased dramatically, and the particles precipitated within minutes (Figure 6, inset). Jia et al. reported a similar increase in size for untreated nanoparticles in the presence of lysozyme.²⁹ Zwitterated nanoparticles, in comparison, maintained a constant hydrodynamic size for 30 h, after which the hydrodynamic radius grew by ca. 20 nm as seen in Figure 6 (see Figures S7 and S8 for correlation functions and size distributions, respectively). He et al.⁴⁶ studied the *in vivo* biodistribution of fluorescent silica nanoparticles with a particle diameter of 45 nm and different surface functionalities. Surfaces terminated with PEG had the longest blood circulation

(43) Bergna, H. E.; Roberts, W. O., Eds.; *Colloidal Silica: Fundamentals and Applications*; CRC Press: Boca Raton, FL, 2006.

(44) Liang, Y.; Hilal, N.; Langston, P.; Starov, V. *Adv. Colloid Interface Sci.* **2007**, *134–35*, 151–166.

(45) Arai, T.; Norde, W. *Colloids Surf.* **1990**, *51*, 1–15.

(46) He, X. X.; Nie, H. L.; Wang, K. M.; Tan, W. H.; Wu, X.; Zhang, P. F. *Anal. Chem.* **2008**, *80*, 9597–9603.

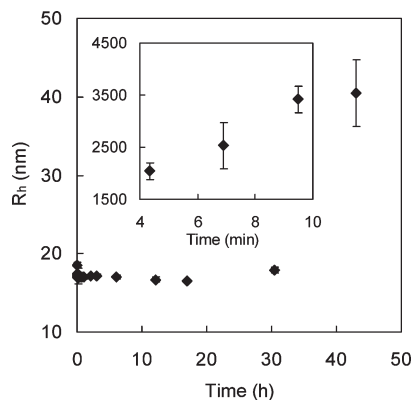


Figure 6. Hydrodynamic radius of $1.7 \mu\text{mol Zwi/m}^2$ zwitterated silica nanoparticle in the presence of lysozyme in PBS (pH 7.4). 3.8 mg of nanoparticles was added to 1 mL of 3.5 mg/mL lysozyme dispersed in 2.5 mL of PBS. Inset shows the hydrodynamic radius for untreated silica nanoparticles under the same conditions.

half-life of 3 ± 0.7 h and were successively delivered to different organs. Our results indicate that the zwitterated nanoparticles resist protein adsorption up to 30 h, suggesting potentially long circulation times *in vivo*. Similar results were observed with polymeric zwitterions,^{28,29} however, to our knowledge, stabilization of silica nanoparticles using nonpolymeric, small organosilane zwitterion has not been reported.

In conclusion, silica nanoparticles were stabilized by treating the surface with a zwitterionic organosiloxane molecule. The addition of the zwitterion did not significantly change the hydrodynamic radius of the nanoparticles, in contrast to conventional surface stabilization using polymers, where an increase in particle size is observed on grafting to the surface. The zwitterated nanoparticles were found to be stable under challenging conditions, such as 3 M NaCl, in 50% FBS, and in the presence of lysozyme, which is positively charged. This surface passivation approach offers an alternative to polymeric stabilization when preserving particle size, especially of nanomaterials in the 3–50 nm range, is so important to *in vivo* uptake, targeting, and circulation behaviors.

Acknowledgment. Dr. Thomas Gedris is acknowledged for his help in solid-state NMR and Dr. Andreas Reisch for his help in ^1H NMR spectra. Dr. Claudius Mundoma is acknowledged for help with dynamic light scattering. We also acknowledge Professor S. P. Armes and Dr. Damien Dupin at the University of Sheffield for zeta potential measurements.

Supporting Information Available: NMR peak assignments, turbidimetry experiments under high salinity conditions, hydrodynamic radii, NMR hydrolysis of zwitterion siloxane, and effect of heating on stability. This material is available free of charge via the Internet at <http://pubs.acs.org>.